ELSEVIER

Biochimica et Biophysica Acta 1480 (2000) 222–234

BIOCHIMICA ET BIOPHYSICA ACTA
BBA

www.elsevier.com/locate/bba

Active site studies of bovine α1→3-galactosyltransferase and its secondary structure prediction

Premal S. Shah [a,1], Frantisek Bizik [a], Rina K. Dukor [b], Pradman K. Qasba [a,*]

[a] *Structural Glycobiology Section, Laboratory of Experimental and Computational Biology, National Cancer Institute, NCI-FCRDC, Room 221, Building 469, Frederick, MD 21702, USA*

[b] *Vysis Inc., Downers Grove, IL, USA*

Received 15 November 1999; received in revised form 28 March 2000; accepted 30 March 2000

Abstract

The catalytic domain of bovine α1→3-galactosyltransferase (α3GalT), residues 80–368, have been cloned and expressed, in *Escherichia coli*. Using a sequential purification protocol involving a Ni^{2+} affinity column followed by a UDP-hexanolamine affinity column, we have obtained a pure and active protein from the soluble fraction which catalyzes the transfer of galactose (Gal) from UDP-Gal to *N*-acetyllactosamine (LacNAc) with a specific activity of 0.69 pmol/min/ng. The secondary structural content of α3GalT protein was analyzed by Fourier transform infrared (FTIR) spectroscopy, which shows that the enzyme has about 35% β-sheet and 22% α-helix. This predicted secondary structure content by FTIR spectroscopy was used in the protein sequence analysis algorithm, developed by the Biomolecular Engineering Research Center at Boston University and Tasc Inc., for the assignment of secondary structural elements to the amino acid sequence of α3GalT. The enzyme appears to have three major and three minor helices and five sheet-like structures. The studies on the acceptor substrate specificity of the enzyme, α3GalT, show that in addition to LacNAc, which is the natural substrate, the enzyme accepts various other disaccharides as substrates such as lactose and Gal derivatives, β-*O*-methylgalactose and β-D-thiogalactopyranoside, albeit with lower specific activities. There is an absolute requirement for Gal to be at the non-reducing end of the acceptor molecule which has to be β1→4-linked to a second residue that can be more diverse in structure. The kinetic parameters for four acceptor molecules were determined. Lactose binds and functions in a similar way as LacNAc. However, β-*O*-methylgalactose and Gal do not bind as tightly as LacNAc or lactose, as their K_{ia} and K_A values indicate, suggesting that the second monosaccharide is critical for holding the acceptor molecule in place. The 2′ and 4′ hydroxyl groups of the receiving Gal moiety are important in binding. Even though there is large structural variability associated with the second residue of the acceptor molecule, there are constraints which do not allow certain Gal-R sugars to be good acceptors for the enzyme. The β1→4-linked residue at the second position of the acceptor molecule is preferred, but the interactions between the enzyme and the second residue are likely to be non-specific.

Keywords: Glycosyltransferase; α1→3-Galactosyltransferase; Fourier transform infrared spectroscopy

1. Introduction

Galactosyltransferases (GTs) catalyze the transfer of galactose (Gal) from uridine-5′-diphospho-α-galactose (UDP-Gal) to various monosaccharides and

* Corresponding author. Fax: +1-301-846-7149; E-mail: qasba@helix.nih.gov

[1] Present address: Division of Biochemistry, California Institute of Technology, Pasadena, CA 91125, USA.

0167-4838/00/$ – see front matter
PII: S0167-4838(00)00074-1

oligosaccharides. Several GTs exist, each being unique in the type of linkage it generates upon the transfer of Gal, with the most common linkages observed being 1→3 and 1→4. In addition, the configuration of the anomeric carbon of Gal introduces even more variety into the types of glycosidic linkages formed so that the following types of linkages can occur: α1→4, β1→4, α1→3 and β1→3. Bovine mammary gland β1→4-galactosyltransferase (β4GalT) was the first GT to be cloned and studied [1–5], which was followed by the cloning of α1→3-galactosyltransferase (α3GalT) [6–8].

The α3GalT catalyzes the transfer of Gal from UDP-Gal to *N*-acetyllactosamine (Galβ1→4GlcNAc, LacNAc), producing the trisaccharide Galα1→3Galβ1→4GlcNAc. Unlike the β4GalT reaction, in which the configuration at the C1 atom of Gal is inverted, the α3GalT reaction retains the configuration at the C1 atom. The β4GalT has been extensively studied for its donor and acceptor specificities [9–12] and is stimulated by the modifier protein α-lactalbumin for the transfer of Gal to glucose (Glc) [13,14] and references reviewed in [15]. The α3GalT is unresponsive to α-lactalbumin. The enzyme purified from calf thymus [16,17] and produced by recombinant methods [18–20], has been previously analyzed for its substrate specificity. In addition to its preferred disaccharide, LacNAc, α3GalT is unique amongst other GTs in that it appears to accept several substrates [16,19]. The two enzymes, α3GalT and β4GalT, show very little sequence similarity except in a short stretch of sequence within their catalytic domains [6,21].

The α3GalT enzyme is responsible for the production of the α-galactosyl epitope in the sequence Galα1→3Galβ1→4GlcNAc of many mammalian oligosaccharides. This enzyme is not expressed in humans, apes and old world primates due to gene inactivation by two frame shift mutations [6,22–24]. Humans, however, express an enzyme that transfers Gal only to α1→2-fucosylated substrate, Fucα1→2Gal, producing the human B antigen, Galα1→3(Fucα1→2)Gal. The presence of the α-galactosyl epitope in the sequence Galα1→3-Galβ1→4GlcNAc-R, present on the surface of most mammalian endothelial cells leads to hyperacute rejection of the transplant during xenotransplantation due to reaction with anti-α-galactosyl epitope antibodies found in humans, apes and other old world primates [25]. These antibodies, in humans, are produced under normal conditions in response to bacteria which reside in the gastrointestinal tract and display α-galactosyl-like epitopes [26].

We have cloned, expressed and purified the bovine α3GalT and examined the nature of its active site. Using various substrates as acceptors we have correlated the specific activity of the enzyme with the preferred conformation of the substrates derived by molecular dynamic (MD) simulations. We have also utilized Fourier transform infrared (FTIR) spectroscopy to determine the secondary structure content of α3GalT. Using the protein sequence analysis (PSA) algorithm, developed by the Biomolecular Engineering Research Center at Boston University and Tasc Inc., along with the predicted secondary structure content of the protein by FTIR analysis, we have assigned the secondary structural elements to the primary sequence.

2. Materials and methods

2.1. Materials

The pET23a vector, His-Bind resin and HMS174(DE3) cells were purchased from Novagen. The site-directed mutagenesis kit and BMH71-18*mut*S cells were from Clontech. DH5α supercompetent cells were from Life Technologies. Taq DNA polymerase and polymerase chain reaction (PCR) nucleotide mix were obtained from Boehringer Mannheim. DNA miniprep spin, PCR purification, low melting agarose extraction kits and Tip-100 columns were from Qiagen. Restriction enzymes were from New England Biolabs. Ampicillin, UDP-Gal, UDP-hexanolamine-agarose resin, LacNAc, Gal, melibiose, cellobiose, β-*O*-methylgalactose, Glc, mannose (Man) and α-lactalbumin were obtained from Sigma. Lactulose and lactose were from Fluka. Human blood group H substrate was from Dextra Labs. UDP-[6-^{3}H]galactose was from Amersham. AG 1-X8 resin, chloride form, 200–400 mesh was from Bio-Rad.

The bovine lactating mammary gland cDNA library used to amplify the catalytic domain of α3GalT was from our previous studies [5]. Oligonu-

cleotides were from the recombinant DNA laboratory, National Cancer Institute.

2.2. Amplification of α3GalT catalytic domain

The following primers were used for the PCR amplification of the cDNA region corresponding to amino acids 80–368 of α3GalT, which have been shown to be the minimum number of residues required for its enzymatic activity [27]. 5′Primer: 5′ GAAAGCAAGCTTAAGCTATCGGACTGGTTCAAC 3′; 3′primer 5′ TCAGACATTATTTCTAACCACATTATACTC 3′. Following the PCR amplification, the DNA fragment corresponding to α3GalT was excised from a low melting agarose gel and served as a template for the second PCR amplification with the following primers which introduced a *Bam*HI restriction site and six residue histidine tag on the 5′ end and an *Eco*RI restriction site on the 3′ end of the amplified DNA. 5′Primer: 5′ CGCGGATCCGCGCACCACCACCACCACCACGAAAGCAAGCTTAAG 3′; 3′primer: 5′ CCGGAATTCCGGTCAGACATTATTTCTAACCACATTATA 3′.

The PCR amplified fragment was digested sequentially with *Bam*HI and *Eco*RI and inserted into a pET23a vector, which was also prepared by digestion with the two restriction enzymes in the same manner. The plasmid pET23a-α3GalT-d79 containing the correct insert was identified by restriction analysis and DNA sequencing.

2.3. Site-directed mutagenesis

Site-directed mutagenesis was carried out according to the manufacturer's protocol using Clontech's Site-Directed Mutagenesis Transformer Kit. Construction of the double mutant, K307Q/K308A, was done using pET23a-α3GalT-d79 as the template plasmid (see above). The transformation mixture contained the template plasmid, a selection primer (pNotApa) and the mutagenic primer K307Q/K308A with the following sequence: 5′ pGCTTCAAAGGGATCCTCAAGGACCAGGCAAATGACATAGAAGCCC 3′. This primer also introduces another *Bam*HI restriction site in the plasmid which was used for screening for the incorporated mutation. The mutation was further confirmed by DNA sequence analysis of the insert in the plasmid K307Q/K308A-pET23a-α3GalT-d79.

2.4. Bacterial strains and growth conditions

Bacterial growth and plasmid transformations were performed using standard procedures [28]. Wild type and mutant constructs of α3GalT were expressed in *E. coli* DH5α supercompetent cells. All clones were grown in Luria–Bertani (LB) medium containing 100 μg/ml ampicillin at 37°C as described [28,29]. Clones which were positive for the desired insertion or mutation were transformed into HMS174(DE3) cells as described [29,30].

2.5. Expression and purification of recombinant wild type and mutant proteins

A 100 ml overnight culture of HMS174(DE3) cells containing the desired plasmid was diluted to one liter using LB broth and ampicillin (final concentration was 100 μg/ml). At an OD of 0.7 at A_{600}, isopropyl β-D-thiogalactopyranoside (IPTG) was added to a final concentration of 1 mM to induce protein production. The culture was grown at 37°C for an additional 4 h at which time cells were harvested by centrifugation at $600\times g$ for 10 min. The cells were frozen in a dry ice–ethanol bath for 1.5 h and then allowed to thaw completely. The cells were resuspended in 20 ml equilibration/binding buffer (20 mM Tris–HCl, pH 8.0, 5 mM immidazole, 0.5 M NaCl, 0.2 mg/ml lysozyme) and vigorously shaken for 10 min. DNAse I was added (2 μg/ml) and the cell mixture was shaken at 37°C. The cell lysate was centrifuged at $27\,000\times g$ for 20 min. The supernatant, which contains soluble proteins, was passed through a His-Bind column (Novagen) at 4°C. The column was first charged and washed as per the manufacturer's protocol and then equilibrated with three bed volumes of equilibration/binding buffer. The supernatant was passed through the column twice and subsequently washed with six bed volumes of equilibration/binding buffer. The protein was eluted with six bed volumes of elution buffer (20 mM Tris–HCl, 0.5 M NaCl and 100 mM immidazole).

A UDP-hexanolamine-agarose (Sigma) column was used to further purify the protein. Mn^{2+} was

added (25 mM) to the pooled elutions from the His-Bind column. The column was equilibrated using three bed volumes of equilibration/washing buffer B (25 mM PIPES, 10 mM dithiothreitol, 50 mM $MgCl_2$, 1.0% Triton X-100, 50 mM $MnCl_2$). The protein sample was passed through the column twice and washed with four bed volumes of equilibration/wash buffer B. The protein was eluted from the column with six bed volumes of elution buffer B (25 mM PIPES, 25 mM EDTA, 1 M NaCl) and dialyzed against 20 mM Tris–HCl, pH 7.0 and 150 mM NaCl.

2.6. Enzymatic assay for α3GalT

Reactions were carried out at 37°C for 15 min in a 100 μl volume containing 5 mM $MnCl_2$, 5 mM Tris–HCl (pH 7.0), 50 μM UDP-Gal and 10 mM sugar acceptors. The reaction was terminated by the addition of 200 μl ice-cold water to the incubation mixture and passed through 0.5 ml of AG 1-X8 anion exchange resin (Bio Rad) in a scintillation vial. Next, the resin was washed sequentially with 0.3, 0.4 and 0.5 ml of water. Twenty ml Ecoscint A scintillation solution (National Diagnostics) was added to each vial and the radioactivity counted in a Beckman LS 3801 liquid scintillation counter. One unit of enzyme activity is defined as the amount of enzyme that catalyzes the transfer of 1 μmol of Gal from UDP-Gal to LacNAc at 37°C.

2.7. Kinetic analysis for α3GalT

For kinetic analysis of the enzyme, five different concentrations of the donor, UDP-Gal, in the range of 5 to 75 μM, and six different concentrations of the acceptor sugar were used in a range that allowed for an accurate Michaelis–Menten plot to be derived. Data were analyzed for a two-substrate system using Eq. 1, similar to the method used by Seto et al. [31,32].

$$v = \frac{v[A][B]}{K_{ia}K_B + K_B[A] + K_A[B] + [A][B]} \quad (1)$$

EnzFitter Program, a non-linear curve fitting program for Windows from Biosoft, was used to obtain the kinetic parameters K_A, K_B, K_{ia} and v_{max}, from the fitted curves using the above rate equation.

2.8. Analysis of protein secondary structure by FTIR

Protein was concentrated using Centriprep YM-10 from Millipore by centrifugation at $8000 \times g$ to 6 mg/ml in a buffer containing 20 mM Tris–HCl, pH 7.0 and 150 mM NaCl. Filtrates were saved and used for subtracting the background during spectral analysis. FTIR spectra were measured on the PROTA FTIR-protein analyzer from Bomem, equipped with the Arid-Zone purge system, non-hygroscopic ZnSe beamsplitter and DTGS detector. The spectrometer was continuously purged with dry air. The resolution used was 4 cm^{-1} and all spectra were collected for 25 min. Two different cells were used for measurements. One cell, composed of two CaF_2 windows and a 6 μm mylar spacer (Specac) was assembled, buffer (filtrate) collected and vacuum dried, followed by an acquisition of a protein spectrum. That is, the cell was not taken apart between the measurements of buffer and protein spectra in order to preserve a constant pathlength. The second cell (BioTools), originally designed by Venyaminov et al. [33], is formed between a perfectly flat, optically clear CaF_2 disc and another CaF_2 disc, the center of which had been deepened to form a recessed parallel surface surrounded by a groove. The cell pathlength is 5.3 μm. This cell is assembled and disassembled between the buffer and protein measurements but since no spacer is used, the pathlength reproducibility is very good and can be adjusted by comparing the signal beam spectra. The sample volume for both cells is approximately 10 μl. The H_2O based buffer (filtrate) spectrum was subtracted from the protein spectrum using an automated subtraction algorithm in PROTA [34]. Each sample was measured at least twice.

Secondary structure calculations were done using PROTA's database and programs and are based on the work of Keiderling et al. [35,36]. Second derivative spectra [37] were calculated in PROTA using algorithms developed by Spectrum Square Associates (Ithaca, NY, USA).

2.9. MD simulations of the substrates

The calculations were performed using MacroModel (MacroModel, Columbia University, NY, USA) employing an MM3 force field [38]. MD simulations of β-*O*-methylgalactose, IPTG, lactulose, mellibiose,

LacNAc and lactose were carried out with inclusion of the solvent effect (water solution) utilizing the GB/SA continuum solvation model. The length of MD simulations was 2 ns for each molecule and a constant temperature of 300 K was maintained during the simulations. An integration time step of 1 fs was used and coordinates were saved every picosecond. From saved MD trajectories, several lowest energy conformers were selected and geometries of these conformers were optimized. The lowest energy conformer from optimized structures was used for superposition.

3. Results and discussion

3.1. Construction, expression and purification of recombinant bovine α3GalT

The bacterial clone containing plasmid construct pET23a-α3GalT-d79 was induced to produce α3GalT protein. The sequence of the expressed protein without the six residue histidine tag is shown in Fig. 1. The induced protein in the bacteria remains mostly in the soluble fraction upon cell lysis from where it was purified sequentially on a Ni^{2+}-agarose column and UDP-hexanolamine column and subsequently dialyzed. The yield of the final purified protein was ~3 mg from 1 l culture. Dialysis against 20 mM Tris–HCl (pH 7.0) alone precipitates the protein in a relatively short period of time. After examining the protein on an isoelectric focusing gel (pH 3–10), two bands appear, each band constituting approximately 50% of total observed protein, which are one pH unit apart. In an attempt to obtain only one isoform of the enzyme, the protein from the UDP-hexanolamine column was dialyzed against 150 mM NaCl and 20 mM Tris–HCl, pH 7.0. This gave a single protein band, on both SDS–PAGE and isoelectric focusing gels. In addition, precipitate formation also decreased significantly, indicating that the higher ionic strength favors one isoform over another, most likely the active form since the specific activity of protein in 150 mM NaCl was higher than the sample devoid of NaCl. Therefore, it can be assumed that a dynamic equilibrium is present between two distinct forms of α3GalT which are dependent on salt concentration and as the salt concentration is increased, the active isoform predominates. The FTIR spectrum of the protein sample in low salt concentrations could not be determined due to the aggregation and precipitation of the protein in solution.

The N-terminal sequence of the purified protein showed that after six histidine residues the amino acid sequence ESKLKL appeared, which corre-

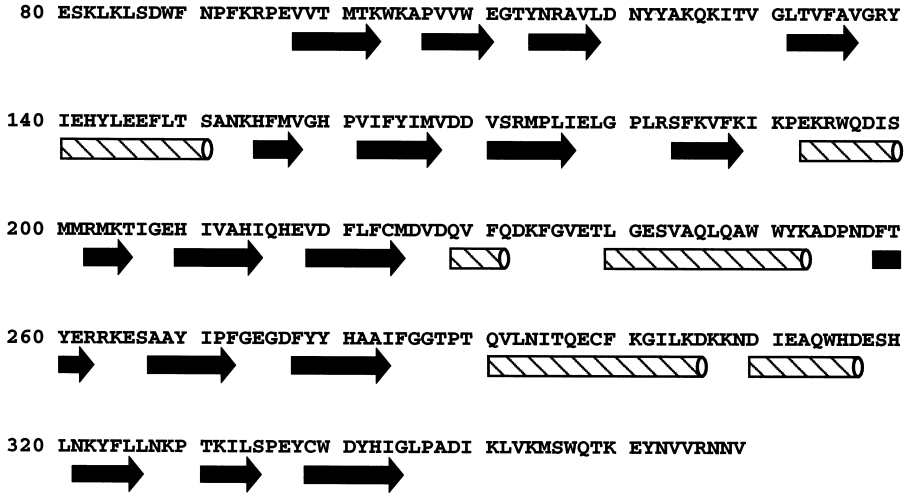

Fig. 1. Sequence of the expressed catalytic domain of bovine α3GalT. Six histidine residues at the amino terminal end of the sequence are not shown. Secondary structure elements are shown under the sequence. Sheets (arrows) and helices (barrels) were assigned based on the PSA algorithm which was fitted using the obtained FTIR results.

sponds to the sequence of α3GalT starting at residue number 80 in Fig. 1. The specific activity of the enzyme is 0.6 U/mg of purified protein, with LacNAc as an acceptor, which is about 1/5 of the activity reported for the recombinant enzyme produced in the baculovirus system [18]. The enzyme purified from calf thymus [16] and the recombinant enzyme produced in *E. coli* by Fang et al. [27] have been shown to have higher activities than reported here or by Joziasse et al. [18]. Since the purified protein in the present study shows a single band on SDS as well as on isoelectric focusing gels (at high salt concentrations) and the salt concentrations can influence the activity of the enzyme (see above), we assume that the differences in the specific activity of the enzyme reported in the literature may be due to the differences in assay conditions used by different groups or due to some modifications introduced on the protein in different expression systems.

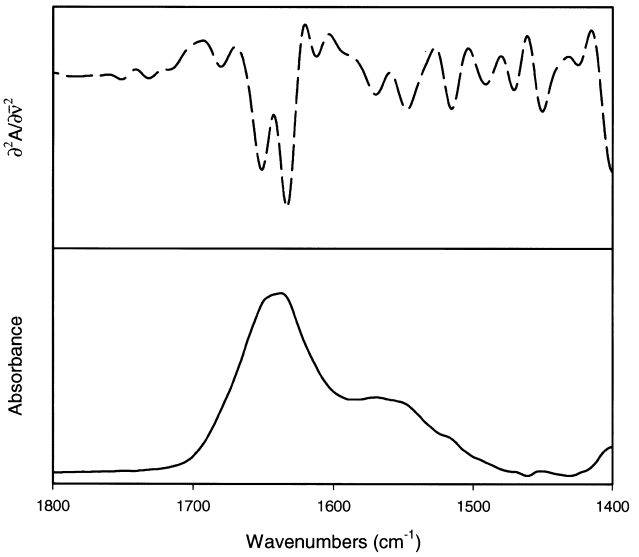

Fig. 2. FTIR spectrum of the recombinant α3GalT showing the absorbance (solid lines) and plot of the second derivative (dashed lines).

3.2. Secondary structure prediction

FTIR spectroscopy has been widely used in studies of secondary structural composition of proteins [39–45]. The technique involves analysis of the conformationally sensitive amide I band, which results primarily due to the stretching vibrations of the protein backbone C=O bond. The nature of the hydrogen bonds involving the C=O and N–H groups of the peptide bond, in addition to the protein backbone geometry, determine the nature of the amide I band [46,47] and, therefore, are indicative of the secondary structures of proteins. Using FTIR spectroscopy and the PSA software (PSA, Biomolecular Engineering Research Center, Boston University and TASC, Reading, MA, USA), we have predicted the secondary structure of α3GalT and applied it to the primary sequence (Fig. 1). The second derivative and FTIR absorbance spectra of the purified α3GalT in 20 mM Tris–HCl, pH 7.0 and 150 mM NaCl are shown in Fig. 2. These spectra are typical of a protein with a high content of mixed α-helix and β-sheet structure. The main bands observed at 1620 and 1660 cm^{-1} are usually assigned to those conformations. The factor analysis results [35] predict the structure to contain approximately 35% β-sheet and 22% α-helical content. These values were used to obtain the cut-off values for the probabilities of each residue being in an α-helix and β-sheet structure predicted with the protein secondary structure algorithm (PSA) [48–50] (Fig. 3). The amino acid residues that had the probabilities above the set cut-offs were assigned their appropriate secondary structure elements (Fig. 1). The secondary structure of the sequence reveals three major helices in addition to three minor ones. There also appear to be five sheet-like structures, consisting of three or four strands each. Of course, the exact nature of the sheets and the number of strands may be inaccurate because the exact fold of the molecule is unknown. Recently, the structure and fold of α3GalT was modeled based on the known structures of the nucleotide sugar-binding domains of proteins in the PDB database [51]. The modeled structure predicts that the enzyme consists of alternating α-helices and β-strands which in most part are in good agreement with the secondary structure predictions based on the spectroscopic data presented, except for the regions of amino acids 200–220 and 259–267. The differences are due to different secondary structure prediction methods used. In the secondary structure prediction by the PSA algorithm we have used the constraints such that the cut-off values for the secondary structure element of a residue fit the overall secondary structure element prediction from the spectroscopic method. This may be the reason that the regions of amino acids 200–220 and

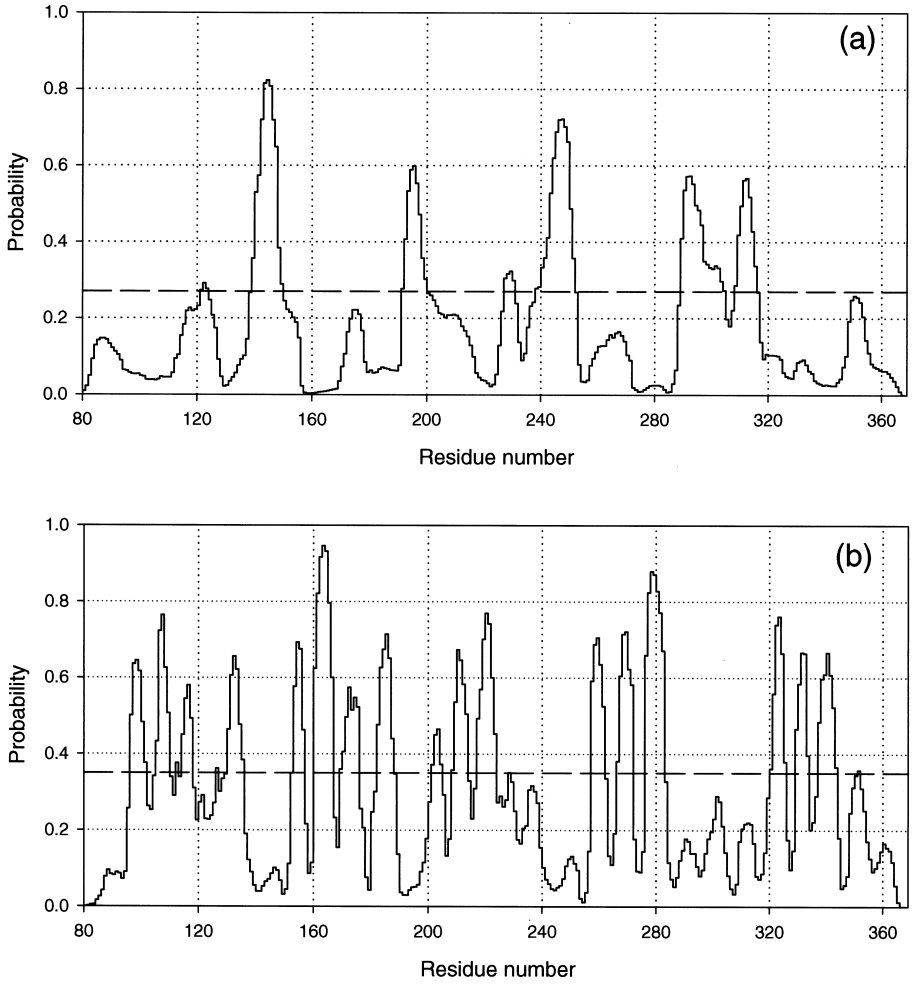

Fig. 3. Probabilities of α3GalT residues being in a α-helix (a) and in a β-strand (b). The probabilities were obtained using PSA software. Cut-off lines (dashed lines) were set based on FTIR prediction of 22% α-helical and 35% β-sheet content, delineating the residues in α-helix and in a β-strand structure.

259–267 have given the structural elements that differ from those reported by Imberty et al. [51].

3.3. Metal dependency of α3GalT

A variety of divalent metal cations can activate α3GalT with different acceptors, albeit at lower rates compared to the preferred manganese (Mn^{2+}) ion (Table 1). When LacNAc is used as a substrate, cobalt (Co^{2+}) is 83% as effective as Mn^{2+}, while iron (Fe^{2+}), cadmium (Cd^{2+}) and magnesium (Mg^{2+}) are less effective. The activation can vary depending on the acceptor used as shown in Table 1. Metal ions, Mg^{2+} and Zn^{2+} are less efficient in activating the enzyme than Mn^{2+} when LacNAc is used as the acceptor and even less efficient when β-*O*-methylgalactose is used as the acceptor.

The use of more than one metal ion is not uncommon to GTs. β4GalT, for example, can use a variety of metal ions in place of the preferred Mn^{2+} ion [52]. The Mn^{2+} saturation curve for the transfer of Gal to LacNAc by α3GalT is sigmoidal. This type of graph shows that there are at least two activating metal binding sites on the enzyme which is concurrent with earlier findings [53].

3.4. Acceptor specificity of α3GalT

The acceptor specificity of bovine α3GalT has been previously studied [16,17,19] and it has been

Table 1
Specific activities of wild type α3GalT using various divalent metal cations

Metal ion	Activity relative to LacNAc (%)	Activity relative to β-*O*-methylgalactose (%)
Mn^{2+}	100	100
Ca^{2+}	2	0
Mg^{2+}	44	4
Cd^{2+}	33	33
Fe^{2+}	24	26
Zn^{2+}	21	7
Co^{2+}	83	52

The concentrations of UDP-Gal and metal ions were, 50 μM and 5 mM, respectively, and acceptors LacNAc and β-*O*-methylgalactose were 10 mM each. Relative activities of 100% correspond to specific activities of 0.61 and 0.11 pmol min^{-1} ng^{-1} for the acceptors LacNAc and β-*O*-methylgalactose, respectively.

shown that the enzyme utilizes a range of sugar acceptors and their derivatives, suggesting that the enzyme has a broad acceptor specificity, just as the enzyme obtained from *Trypanosoma brucei* [20]. It has been suggested that a Gal moiety on the acceptor molecule is an absolute requirement for the transfer of Gal from UDP-Gal by the enzyme. In addition to Gal and its derivatives we have used talose (Tal) and Glc as acceptor molecules to determine which hydroxyl groups are important in binding the Gal residue (Table 2). Since neither Tal nor Glc display any significant activity, it can be inferred that the C2 and C4 hydroxyl groups on Gal are critical for the activity of the enzyme. In addition to the absolute requirement for Gal, the residue on the reducing end of the Gal moiety can be more diverse in structure (Table 2). There appear to be some constraints, however. Lactulose (Galβ1→4Fru) which appears at least spatially to be similar to other highly active substrates (Fig. 4), interacts less favorably with the enzyme (Table 2) which may be due to the steric hindrances caused by the CH_2OH groups on fructose. We also wanted to test if the enzyme was able to accommodate disaccharides containing a linkage other than the β1→4 linkage. Melibiose (Galα1→6Glc) displays only 4% activity compared to LacNAc, suggesting that a disaccharide with β1→4 linkage is a preferred substrate. Additional evidence supporting the importance of the disaccharide linkage is the inability of GlcNAc to stimulate α3GalT activity when Gal and GlcNAc are provided together as the acceptor substrate. This implies that providing the enzyme with both components of a disaccharide is not enough and that the linkage between the anomeric carbon of the first monosaccharide and the second sugar is indeed important.

The superposed minimum energy structures of the substrates that were tested show that in the active substrates C2, C3 and C4 atoms of the β-linked monosaccharide moiety of the disaccharide superimpose and face towards one side of the molecule (Fig. 4), which may contribute to additional interactions with the enzyme. In addition, a hydrophobic

Table 2
Specific activities of various acceptor substrates using wild type α3GalT

Substrate	Activity relative to LacNac (%)
N-Acetyllactosamine (LacNAc)[a]	100
Galβ1→4Glc (lactose)	76
β-*O*-Methylgalactose	22
D-Galactose	9
Glcβ1→4Glc (cellobiose)	0
Glucose	0
N-Acetylglucosamine (GlcNAc)	0
Galα1→6Glc (melibiose)	4
D-Mannose	0
D-Talose	2
Galacturonic acid	0
Fucα1→2Gal (human blood group H)[a]	0
IPTG	63
Galβ1→4Fru (lactulose)	45

Concentrations of UDP-Gal, Mn^{2+} and sugar acceptors were 50 μM, 5 and 10 mM, respectively. Relative activity of 100% corresponds to a specific activity of 0.69 pmol min^{-1} ng^{-1} for the LacNAc acceptor.

[a]The specific activity of the double mutant K307Q/K308A of α3GalT remains the same as for the wild type α3GalT for LacNAc and human blood group H substrate, Fucα1→2Gal.

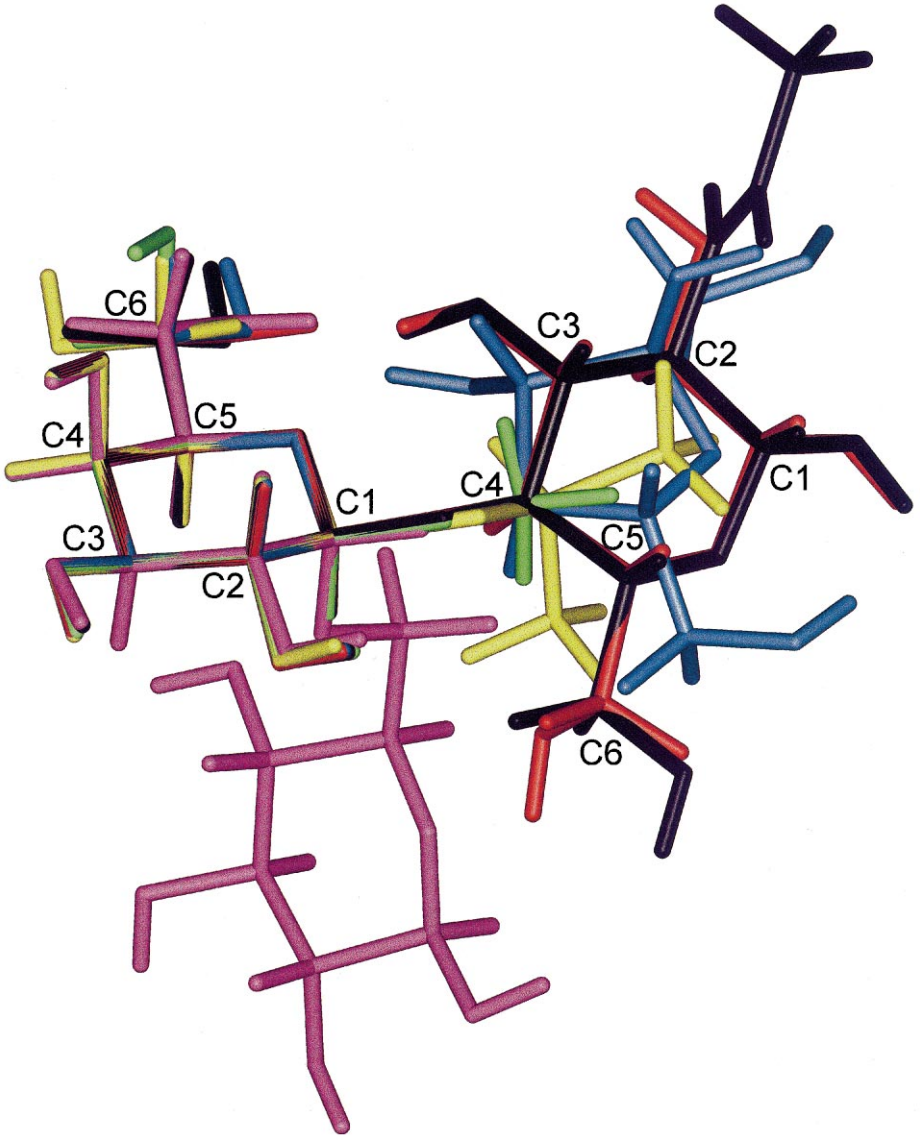

Fig. 4. Superposition of tested acceptor substrates, using the Gal moiety of the oligosaccharides as the reference molecule. Preferred conformations of the substrates were determined by MD simulation and subsequent optimization using MacroModel software. Molecules represented are: LacNAc (black), β-lactose (red), β-*O*-methylgalactose (green), melibiose (pink), IPTG (yellow) and lactulose (blue). Carbon atoms of LacNAc are labeled. The figure was prepared with the program Insight II (Molecular Simulations, San Diego, CA, USA).

patch created by C3H, C5H and $C6H_2$ on the Glc moiety of lactose or GlcNAc moiety of LacNAc, may also be required for interactions with the enzyme. In the same area, a hydrophobic patch is created by the $CH\text{-}(CH_3)_2$ moiety of the IPTG molecule which may contribute to its higher specific activity towards the enzyme compared to Gal or β-*O*-methylgalactose. This suggests that besides the absolute requirement for the Gal moiety, a hydrophobic residue which is linked via a β-glycosidic bond to Gal, that fits in the site adjacent to the Gal binding site on the enzyme, enhances the activity of the enzyme. This hypothesis is in accord with the kinetic data which shows that the true K_m for LacNAc and lactose is several fold lower than for Gal and β-*O*-methylgalactose (Table 3) (see Section 3.5).

Table 3
Kinetic parameters for LacNAc, lactose, β-*O*-methylgalactose and Gal, using wild type α3GalT

Substrate	K_A (mM)	K_B (μM)	K_{ia} (mM)	K_{ib} (μM)	k_{cat} (min^{-1})	k_{cat}/K_A (s^{-1} M^{-1})	k_{cat}/K_B (s^{-1} mM^{-1})
N-Acetyllactosamine	1.1	78	0.04	2.9	38	576	8.1
Lactose	2.1	35	0.3	5.2	17	135	8.1
β-*O*-Methylgalactose	37	15	23	9.4	9	4.1	10
Galactose	1010	53	157	8.3	26	0.43	8.2

K_A and K_B, the true K_m of acceptor and donor, respectively, and K_{ia} and k_{cat} were obtained by two substrate analysis using the primary plots of five concentrations of donor (UDP-Gal) and six concentrations of acceptor and the corresponding secondary plots of the intercepts and slopes. Initial rate conditions were linear with respect to time. A suitable range, one which fell mostly in the linear portion of the Michaelis–Menten plot, for each substrate was identified and used for the primary and secondary plots, as well for the analysis with the EnzFitter Program (Biosoft) using the formula given in Section 2.

3.5. Kinetic parameters for various substrates of α3GalT

The enzymatic mechanism of β4GalT1 has been proposed to be a random equilibrium mechanism [54]. The kinetic mechanism of α3GalT is not known. We have analyzed the steady state kinetic data of α3GalT with LacNAc, lactose, β-*O*-methylgalactose and Gal as acceptor substrates at saturating concentrations of Mn^{2+} (5 mM) in which the concentrations of both UDP-Gal and acceptor substrates were varied (Table 3). Using the equation for a two substrate system (Eq. 1), the true K_m values (K_A) for LacNAc and lactose were determined to be very similar. The K_A value, however, increases 20-fold when β-*O*-methylgalactose is used as the acceptor molecule and almost 500 -fold when Gal is the acceptor. The K_{ia}, the equilibrium dissociation constant for the acceptor molecule, also increases but at a much more dramatic rate. The K_{ia} value for lactose compared to LacNAc increases 10-fold, while the K_{ia} value for β-*O*-methylgalactose and Gal increase by 600- and 4000-fold, respectively. This suggests that the binding of UDP-Gal to the enzyme prior to acceptor binding aids in binding the acceptor more tightly to the enzyme. Furthermore, the UDP-Gal binding most likely affects the binding of the second monosaccharide moiety of a disaccharide. The turnover number, k_{cat}, can be influenced by rate-limiting substrate binding or the product release step and, therefore, the specificity constants, k_{cat}/K_A and k_{cat}/K_B which combine rate and binding, are a more accurate measure of the efficiency of a reaction. Our results suggest that the second residue in a disaccharide is critical for binding and the resulting catalytic efficiency as is evident by the sharp decline in k_{cat}/K_A, using Gal as the acceptor. Although the acceptor specificity of α3GalT is broad, the binding and the catalytic machinery of the enzyme are indeed affected by interchanging various acceptor substrates. The K_B value, the true K_m for UDP-Gal at infinite concentrations of the acceptor and K_{ib}, the equilibrium dissociation constant for UDP-Gal, do not change as dramatically as the acceptor binding parameters, indicating that the acceptor binding site is not associated with the donor binding site and that the effect of UDP-Gal binding on the acceptor binding site is more profound than the effect of the acceptor binding site on the donor site. This is also evident when the specificity constant, k_{cat}/K_B, is compared for the four different substrates. The range is 8–10 s^{-1} mM^{-1}, indicating that the various acceptor sugars do not hinder UDP-Gal binding or alter its role in catalysis.

3.6. Mutation of the DKKN sequence in α3GalT

The DKKN sequence, present in α3GalT (Fig. 1) and in β4GalT1, has been implicated in substrate binding of these enzymes [21]. The corresponding sequence in the human blood group B enzyme is DQAN. Based on our secondary structure prediction (Fig. 3), this sequence in α3GalT is located at the end of a helix, near a turn, which is a common location for substrate binding motifs of many enzymes. We created a double mutant of α3GalT, K307Q/K308A, where Lys-307 was mutated to Gln-307, and Lys-308 to Ala-308, with a hope that α3GalT may accept human blood group H substrate (Fucα1→2Gal) as the acceptor molecule and thereby

acquire a property of the human blood group B enzyme. However, both enzymes, the double mutant K307Q/K308A and the wild type α3GalT, did not show any activity towards the substrate Fucα1→2Gal. On the other hand, the mutant enzyme had the same activity towards LacNAc as the wild type, suggesting that KK residues of DKKN sequence are not involved in the sugar acceptor binding site. Furthermore, these results show that the C2 hydroxyl group on Gal has to be free and is critical for the activity of the enzyme.

Acknowledgements

The authors would like to thank members of the laboratory, Dr. Boopathy Ramakrishnan and Dr. Elizabeth Boeggeman for their helpful discussion and advice during this work. P.S.S would like to thank D.J. Patel for continued motivation and inspiration.

References

[1] R.N. Russo, N.L. Shaper, J.H. Shaper, Bovine beta 1–4-galactosyltransferase: two sets of mRNA transcripts encode two forms of the protein with different amino-terminal domains. In vitro translation experiments demonstrate that both the short and the long forms of the enzyme are type II membrane-bound glycoproteins, J. Biol. Chem. 265 (1990) 3324–3331.

[2] A.S. Masibay, P.K. Qasba, Expression of bovine beta-1,4-galactosyltransferase cDNA in COS-7 cells, Proc. Natl. Acad. Sci. USA 86 (1989) 5733–5737.

[3] G. D'Agostaro, B. Bendiak, M. Tropak, Cloning of cDNA encoding the membrane-bound form of bovine beta-1,4-galactosyltransferase, Eur. J. Biochem. 183 (1989) 211–217.

[4] N.L. Shaper, J.H. Shaper, J.L. Meuth, J.L. Fox, H. Chang, I.R. Kirsch, G.F. Hollis, Bovine galactosyltransferase: identification of a clone by direct immunological screening of a cDNA expression library, Proc. Natl. Acad. Sci. USA 83 (1986) 1573–1577.

[5] H. Narimatsu, S. Sinha, K. Brew, H. Okayama, P.K. Qasba, Cloning and sequencing of cDNA of bovine *N*-acetylglucosamine (beta 1–4)galactosyltransferase, Proc. Natl. Acad. Sci. USA 83 (1986) 4720–4724.

[6] D.H. Joziasse, J.H. Shaper, D.H. Van den Eijnden, A.J. Van Tunen, N.L. Shaper, Bovine alpha-1,3-galactosyltransferase: isolation and characterization of a cDNA clone. Identification of homologous sequences in human genomic DNA, J. Biol. Chem. 264 (1989) 14290–14297.

[7] T.R. Henion, B.A. Macher, F. Anaraki, U. Galili, Defining the minimal size of catalytically active primate alpha 1,3 galactosyltransferase structure–function studies on the recombinant truncated enzyme, Glycobiology 4 (1994) 193–201.

[8] A. Katayama, H. Ogawa, K. Kadomatsu, N. Kurosawa, T. Kobayashi, N. Kaneda, K. Uchimura, I. Yokoyama, T. Muramatsu, H. Takagi, Porcine alpha-1,3-galactosyltransferase: full length cDNA cloning, genomic organization, and analysis of splicing variants, Glycoconjug. J. 15 (1998) 583–589.

[9] J.F. Morrison, K.E. Ebner, Studies on galactosyltransferase. Kinetic investigations with *N*-acetylglucosamine as the galactosyl group acceptor, J. Biol. Chem. 246 (1971) 3977–3984.

[10] J.F. Morrison, K.E. Ebner, Studies on Galactosyltransferase. Kinetic investigations with glucose as the galactosyl group acceptor, J. Biol. Chem. 246 (1971) 3985–3991.

[11] L.J. Berliner, M.E. Davis, K.E. Ebner, T.A. Beyer, J.E. Bell, The lactose synthase acceptor site: a structural map derived from acceptor studies, Mol. Cell Biochem. 62 (1984) 37–42.

[12] M.M. Palcic, O. Hindsgaul, Flexibility in the donor substrate specificity of beta 1,4-galactosyltransferase application in the synthesis of complex carbohydrates, Glycobiology 1 (1991) 205–209.

[13] U. Brodbeck, W.L. Denton, N. Tanahashi, K.E. Ebner, The isolation and identification of the B protein of lactose synthetase as alpha-lactalbumin, J. Biol. Chem. 242 (1967) 1391–1397.

[14] K. Brew, T.C. Vanaman, R.L. Hill, The role of alpha-lactalbumin and the A protein in lactose synthetase: a unique mechanism for the control of a biological reaction, Proc. Natl. Acad. Sci. USA 59 (1967) 491–497.

[15] P.K. Qasba, S. Kumar, Molecular divergence of lysozymes and alpha-lactalbumin, Crit. Rev. Biochem. Mol. Biol. 32 (1997) 255–306.

[16] W.M. Blanken, D.H. Van den Eijnden, Biosynthesis of terminal Gal-alpha1–3Gal-beta1–4GlcNAc-R oligosaccharide sequences on glycoconjugates, J. Biol. Chem. 260 (1985) 12927–12934.

[17] K. Sujino, C. Malet, O. Hindsgaul, M.M. Palcic, Acceptor hydroxyl group mapping for calf thymus alpha-(1–3)-galactosyltransferase and enzymatic synthesis of alpha-D-Galp-(1–3)-beta-D-Galp-(1–4)-beta-D-GlcpNAc analogs, Carbohydr. Res. 305 (1998) 483–489.

[18] D.H. Joziasse, N.L. Shaper, L.S. Salyer, D.H. Van den Eijnden, A.C. van der Spoel, J.H. Shaper, Alpha1–3-Galactosyltransferase: the use of recombinant enzyme for the synthesis of alpha-galactosylated glycoconjugates, Eur. J. Biochem. 191 (1990) 75–83.

[19] C.L.M. Stults, B.A. Macher, R. Bhatti, O.P. Srivastava, O. Hindsgaul, Characterization of the substrate specificity of alpha1,3galactosyltransferase utilizing modified *N*-acetyllactosamine disaccharides, Glycobiology 9 (1999) 661–668.

[20] S. Pingel, U. Rheinweiler, V. Kolb, M. Duszenko, Purification and characterization of an alpha-galactosyltransferase from *Trypanosoma brucei*, Biochem. J. 338 (1999) 545–551.

[21] S. Yadav, K. Brew, Identification of a region of UDP-galactose:*N*-acetylglucosamine beta 4-galactosyltransferase involved in UDP-galactose binding by differential labeling, J. Biol. Chem. 265 (1990) 14163–14169.
[22] U. Galili, S.B. Shohet, E. Kobrin, C.L.M. Stults, B.A. Macher, Man, apes, and old world monkeys differ from other mammals in the expression of α-galactosyl epitopes on nucleated cells, J. Biol. Chem. 263 (1988) 17755–17762.
[23] R.D. Larsen, C.A. Rivera-Marrero, L.K. Ernst, R.D. Cummings, J.B. Lowe, Frameshift and nonsense mutations in a human genomic sequence homologous to a murine UDP-Gal:beta-D-Gal(1,4)-D-GlcNAc alpha(1,3)-galactosyltransferase cDNA, J. Biol. Chem. 265 (1990) 7055–7061.
[24] D.H. Joziasse, J.H. Shaper, E.W. Jabs, N.L. Shaper, Characterization of an alpha1–3-galactosyltransferase homologue on human chromosome 12 that is organized as a processed pseudogene, J. Biol. Chem. 266 (1991) 6991–6998.
[25] D.K. Cooper, E. Koren, R. Oriol, Oligosaccharides and discordant xenotransplantation, Immunol. Rev. 141 (1994) 31–58.
[26] U. Galili, R.E. Mandrell, R.M. Hamadeh, S.B. Shohet, J.M. Griffiss, Interaction between human natural anti-alpha-galactosyl immunoglobulin G and bacteria of the human flora, Infect. Immun. 56 (1988) 1730–1737.
[27] J. Fang, J. Li, X. Chen, Y. Zhang, J. Wang, Z. Guo, W. Zhang, L. Yu, K. Brew, P.G. Wang, Highly efficient chemoenzymatic synthesis of alpha-galactosyl epitopes with a recombinant alpha(1–3)-galactosyltransferase, J. Am. Chem. Soc. 120 (1998) 6635–6638.
[28] F.M. Ausubel, R. Brent, R.E. Kinstom, D.D. Moore, J.A. Smith, J.G. Seidman, K. Struhl, Current Protocols in Molecular Biology, 1987.
[29] E.E. Boeggeman, P.V. Balaji, N. Sethi, A.S. Masibay, P.K. Qasba, Expression of deletion constructs of bovine beta-1,4-galactosyltransferase in *Escherichia coli*: importance of Cys134 for its activity, Protein Eng. 6 (1993) 779–785.
[30] E.E. Boeggeman, P.V. Balaji, P.K. Qasba, Functional domains of bovine beta-1,4 galactosyltransferase, Glycoconjug. J. 12 (1995) 865–878.
[31] N.O. Seto, M.M. Palcic, C.A. Compston, H. Li, D.R. Bundle, S.A. Narang, Sequential interchange of four amino acids from blood group B to blood group A glycosyltransferase boosts catalytic activity and progressively modifies substrate recognition in human recombinant enzymes, J. Biol. Chem. 272 (1997) 14133–14138.
[32] N.O. Seto, C.A. Compston, S.V. Evans, D.R. Bundle, S.A. Narang, M.M. Palcic, Donor substrate specificity of recombinant human blood group A, B and hybrid A/B glycosyltransferases expressed in *Escherichia coli*, Eur. J. Biochem. 259 (1999) 770–775.
[33] S.Y. Venyaminov, F.G. Prendergast, Water (H_2O and D_2O) molar absorptivity in the 1000–4000 cm^{-1} range and quantitative infrared spectroscopy of aqueous solutions, Anal. Biochem. 248 (1997) 234–245.
[34] F. Dousseau, M. Therrien, M. Pezolet, On the spectral subtraction of water from the FTIR spectra of aqueous solutions of proteins, Appl. Spectrosc. 43 (1989) 538–542.
[35] T.A. Keiderling, Protein structural studies using vibrational circular dichroism spectroscopy, in: H.A. Havel (Ed.), Spectroscopic Methods for determining Protein Structure in Solution, VCH, New York, 1996, pp. 163–189.
[36] P. Pancoska, S.C. Yasui, T.A. Keiderling, Statistical analyses of the vibrational circular dichroism of selected proteins and relationship to secondary structures, Biochemistry 30 (1991) 5089–5103.
[37] J.K. Kauppinen, D.J. Moffatt, H.H. Mantsch, D.G. Cameron, Fourier self-deconvolution: a method for resolving intrinsically overlapped bands, Appl. Spectrosc. 35 (1981) 271–276.
[38] N.L. Allinger, Y.H. Yuh, J.H. Lii, Molecular mechanics. The MM3 force field for hydrocarbons. 1, J. Am. Chem. Soc. 111 (1989) 8551–8556.
[39] H. Susi, D.M. Byler, Resolution-enhanced Fourier transform infrared spectroscopy of enzymes, Methods Enzymol. 130 (1986) 290–311.
[40] W.K. Surewicz, H.H. Mantsch, New insight into protein secondary structure from resolution-enhanced infrared spectra, Biochim. Biophys. Acta 952 (1988) 115–130.
[41] W.K. Surewicz, H.H. Mantsch, D. Chapman, Determination of protein secondary structure by Fourier transform infrared spectroscopy a critical assessment, Biochemistry 32 (1993) 389–394.
[42] S.J. Prestrelski, D.M. Byler, M.N. Liebman, Generation of a substructure library for the description and classification of protein secondary structure. II. Application to spectra-structure correlations in Fourier transform infrared spectroscopy, Proteins 14 (1992) 440–450.
[43] J.L. Arrondo, A. Muga, J. Castresana, F.M. Goni, Quantitative studies of the structure of proteins in solution by Fourier-transform infrared spectroscopy, Prog. Biophys. Mol. Biol. 59 (1993) 23–56.
[44] A. Dong, P. Huang, W.S. Caughey, Protein secondary structures in water from second-derivative amide I infrared spectra, Biochemistry 29 (1990) 3303–3308.
[45] P. Pancoska, L. Wang, T.A. Keiderling, Frequency analysis of infrared absorption and vibrational circular dichroism of proteins in D_2O solution, Protein Sci. 2 (1993) 411–419.
[46] T. Miyazawa, E.R. Blout, The infrared spectra of polypeptides in various conformations: amide I and II bands, J. Am. Chem. Soc. 83 (1961) 712–719.
[47] S. Krimm, J. Bandekar, Vibrational spectroscopy and conformation of peptides, polypeptides, and proteins, Adv. Protein. Chem. 38 (1986) 181–364.
[48] C.M. Stultz, J.V. White, T.F. Smith, Structural analysis based on state-space modeling, Protein Sci. 2 (1993) 305–314.
[49] C.M. Stultz, R. Nambudripad, R.H. Lathrop, J.V. White, Predicting protein structure with probabilistic models, in: N. Allewell, C. Woodward (Eds.), Advances in Molecular and Cell Biology, JAI Press, Greenwich, 1997, pp. 447–506.
[50] J.V. White, C.M. Stultz, T.F. Smith, Protein classification by

stochastic modeling and optimal filtering of amino-acid sequences, Math. Biosci. 119 (1994) 35–75.
[51] A. Imberty, C. Monier, E. Bettler, S. Morera, P. Freemont, M. Sippl, H. Flockner, W. Ruger, C. Breton, Fold recognition study of alpha3-galactosyltransferase and molecular modeling of the nucleotide sugar-binding domain, Glycobiology 9 (1999) 713–722.
[52] J.T. Powell, K. Brew, Metal ion activation of galactosyltransferase, J. Biol. Chem. 251 (1976) 3645–3652.
[53] Y. Zhang, M. Arana, K. Brew, High yield expression in *E. coli*, kinetic characterization and mutagenesis study of UDP-Gal:Galβ1–4GlcNAc α1–3, galactosyltrasferase, in: 3rd Annual Conference of the Society for Glycobiology, Abstract # 132, Baltimore, MD, 1998.
[54] J.E. Bell, T.A. Beyer, R.L. Hill, The kinetic mechansim of bovine milk galactosyltransferase. The role of alpha-lactalbumin, J. Biol. Chem. 251 (1976) 3003–3013.